


Probabilistic seismic hazard assessment in the northeastern part of Algeria

Mahmoud Hamlaoui¹  · K. Vanneste² · K. Baddari³ · L. Louail⁴ · B. Vlemingckx² · A. Demdoum¹

Received: 23 August 2016 / Accepted: 27 April 2017 / Published online: 1 June 2017
© Saudi Society for Geosciences 2017

Abstract This work involves updating the evaluation of seismic hazard in Northeast Algeria by a probabilistic approach. This reassessment attempts to resolve inconsistencies between seismic zoning in regional building codes and is further motivated by the need to refine the input data that are used to evaluate seismic hazard scenarios. We adopted a seismotectonic model that accounts for differences in interpretations of regional seismicity. We then performed a probabilistic assessment of regional seismic hazard in Northeast Algeria. Based on a homogeneous earthquake catalog and geological and seismotectonic data gathered in the first part of the study, a seismotectonic zoning map was created and seven risk areas were identified. For each area, peak ground acceleration hazard maps were produced. Details of the calculations are provided, including hazard curves at periods of 0.1, 0.2, 0.33, 0.5, 1.0, and 2.0 s and uniform hazard spectra at urban locations in the area, including Sétif, Constantine, Kherrata, Bejaia, and Jijel.

Keywords Area source · Seismic hazard · Probabilistic approach · Peak ground acceleration · Algeria

Introduction

Algeria overlies the region of convergence between the African and Eurasian plates, which results in a remarkably high rate of seismic activity in the northeast of the country (Fig. 1). Hundreds of tremors recorded during the last century have been strongly felt, and several have been damaging, including the $M_s = 6.0$ Constantine earthquake of 27 October 1985 and the $M = 5.4$ Beni-Ouartilane earthquake of 11 October 2000. This history shows that this region of Algeria is exposed to significant seismic risk.

The remainder of this paper is organized as follows. In the “[Seismotectonic context of Northeast Algeria](#)” section, we introduce the seismotectonic context of northern and Northeast Algeria, describing the historic seismicity. An earthquake catalog is compiled in the “[Seismicity catalogue](#)” section, and source areas are defined in “[Definition of the seismic source areas](#)” section, and in the “[Choice of ground motion attenuation relationships](#)” section, we choose the ground motion prediction equations for estimating the seismic hazard. The Gutenberg–Richter parameters for each source region are calculated in the “[Results](#)” section. Finally, the results are presented as hazard maps in the “[Discussion and conclusions](#)” section.

✉ Mahmoud Hamlaoui
hamlaouis@univ-setif.dz

¹ Physics Department, Faculty of Science, University of Setif1, Sétif, Algeria

² Seismology Section, Royal Observatory of Belgium (ROB), Uccle, Belgium

³ Seismological Laboratory, Faculty of Hydrocarbon and Chemistry, University of Boumerdes, Boumerdès, Algeria

⁴ Department of Geology, University of Setif1, Sétif, Algeria

Seismotectonic context of Northeast Algeria

Many authors have investigated the tectonics of Northeast Algeria (e.g., McKenzie 1972, Bounif et al. 1987, Aoudia and Meghraoui 1995, Harbi (2006), etc.). Based on these works, the region can be divided into four distinct morphostructural domains: the inner domain, the tell (Tellian Atlas), the high plateaus, and the Saharan Atlas.

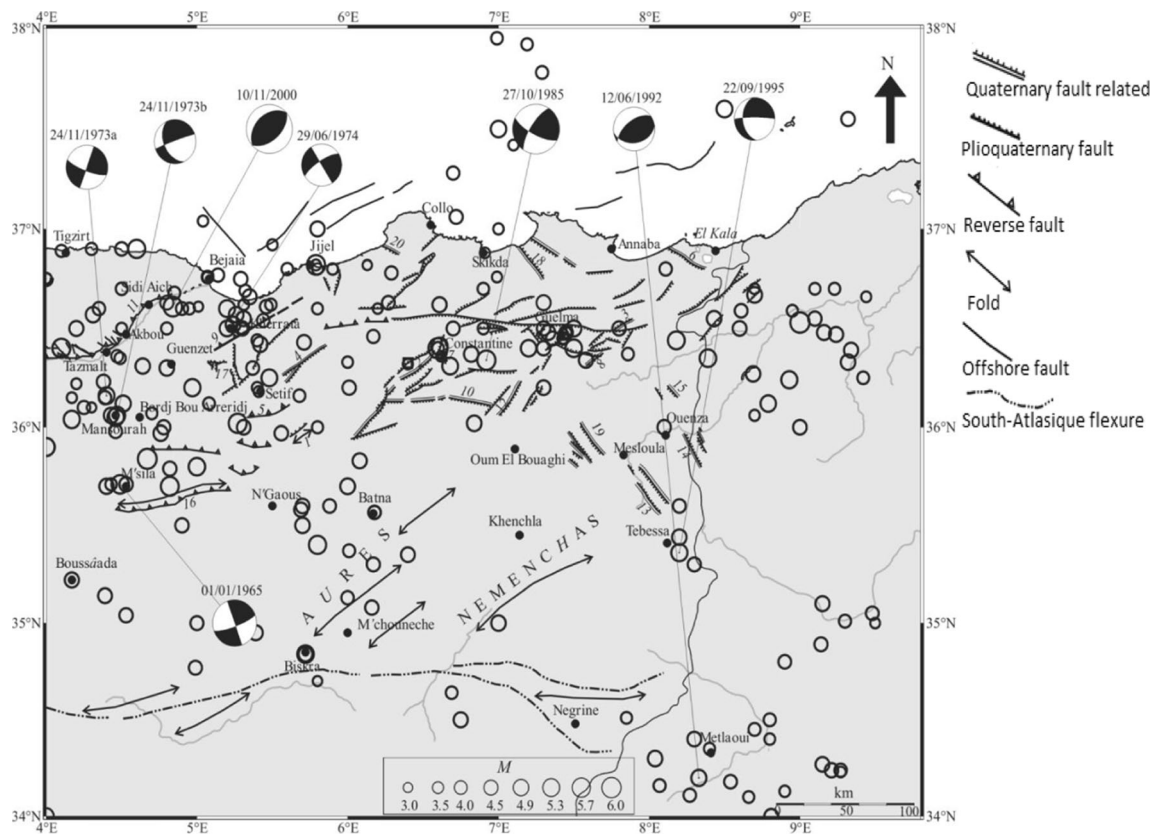


Fig. 1 Seismotectonic map of Northeastern Algeria, showing active and potentially active faults. *a* Quaternary fault related to hydrothermal springs. *b* Plioquaternary fault. *c* Reverse fault. *d* Fold. *e* Offshore fault. *f* South-atlasique flexure. 1 Quaternary anticline of Djebel Tella. 2 AinSmara fault. 3 Bouchegouf fault. 4 Fault of northern Djemila. 5 Fault of Djebel Youcef. 6 Fault of Rosa Cape. 7 Constantine faults. 8

Hammam Bailis fault. 9 Kherrata fault. 10 Sigus fault. 11 Tazmalt-Mechdallah fault. 12 Tamlouka fault. 13 Mesloula fault trough. 14 Ouenza fault trough. 15 Taoura fault trough. 16 Fault-related fold of Chott El Hammam. 17 Network of Guergour-Anini. 18 Fault of Djebel Safia. 19 Terraguelt fault trough (in Harbi et al. 2003)

Recent tectonics in the Tellian Atlas have been dominated by compressive deformation. The distribution of tectonic structures of Plioquaternary allows to distinguish two groups in Tellian Atlas: the north-east of Tellian Atlas with major dextral strike-slip globally trending E-W and forming in its eastern prolongation the Guelma basin. Further to the west, from the meridian of Kherrata, the inverse character takes over, and this recent tectonic regime is marked by the appearance of NE-SW-oriented fold-faults to replay sinistre. The latter area includes the Hodna, the Kherrata area, the Soummam, and especially the Mitidja and Chelif Basins of Central and Western Algeria. Active tectonic processes here are responsible for moderate to large historic and instrumental earthquakes, including the $M_s = 6.0$ Constantine earthquake of 27 October 1985 and the $M_s = 7.3$ EI Asnam earthquake of 10 October 1980 (Meghraoui 1988; Aoudia et al. 2000; Harbi et al. 2003). Figure 1 shows a seismotectonic synthesis of the study area.

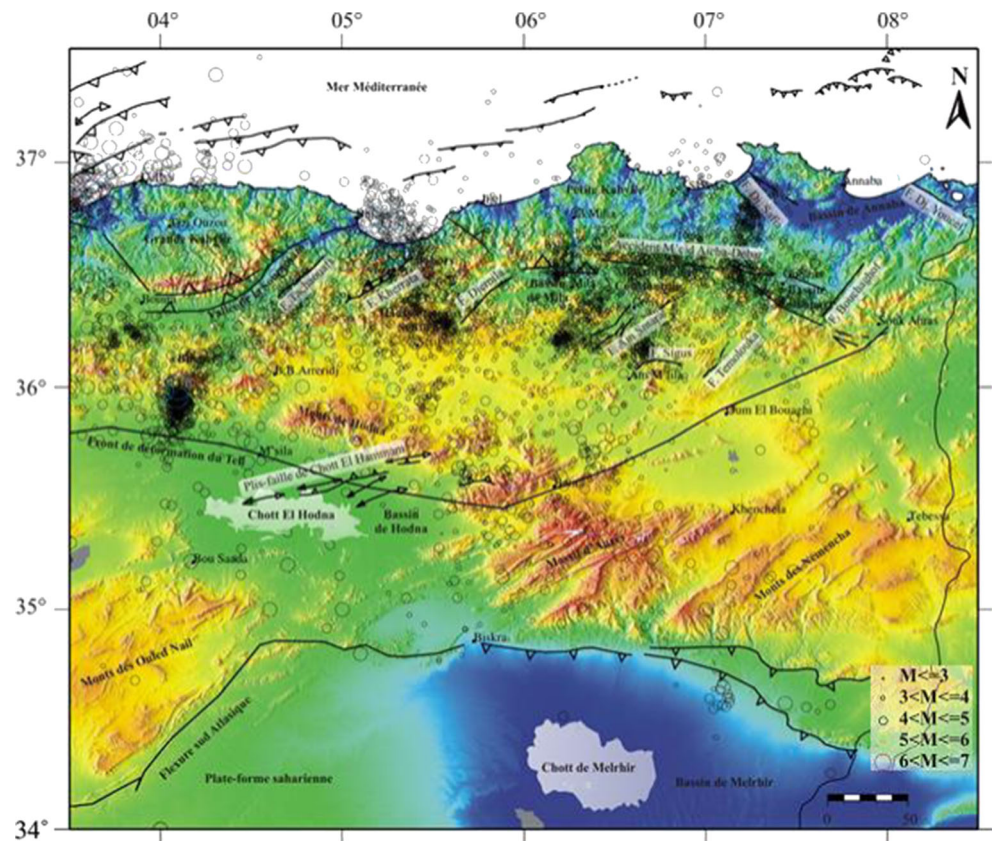
An examination of the seismicity map of Northeast Algeria (Fig. 2) reveals that a majority of earthquakes are located along potentially active faults. It is also notable that seismicity is almost entirely distributed across

the northern part of the study area. The distribution of epicenters follows two major trends: the first runs E-W, parallel to the coast; the second, trending NE-SW, perfectly matches the mapped tectonic features as well as the directions of the respective isoseist of the major earthquakes in the study region (Benhallou 1985; Benouar and Perkins 1993; Mokrane et al. 1994; Harbi et al. 2003).

Methodology

The management of seismic risk in a region begins with a quantitative assessment of the seismic hazard. The latter is generally based on probabilistic or deterministic approaches established through observations of the frequency of historic events and their effects at the surface. The goal of probabilistic seismic hazard analysis is to quantify the likelihood of exceeding a set of acceleration values at a given site based on all possible earthquake scenarios. The methodology applied in this study is based on widely accepted concepts introduced by Cornell (1968) and McGuire (1976).

Fig. 2 Seismicity map of northeastern of Algeria for the period from 1850 to 2015



As stated in a catalog of seismicity (Harbi et al. 2010), seismic activity in this part of Algeria is diffuse, with a moderate activity rate and rare damaging earthquakes (Fig. 2). These limitations do not allow for immediate identification of active structures; moreover, the expected size and recurrence intervals of strong earthquakes remain poorly investigated. With such an incomplete picture of the seismicity, other data resources, including surface geology and geodesy, must be used to quantify the seismic hazard.

Over the past few years, several techniques have been developed to estimate the seismic hazard, including software such as EQRISK (McGuire 1976) and SEISRISK III (Bender 1987). In this study, CRISIS 2007 v7.6 (Ordaz et al. 2007) was used to assess seismic hazard in Northeast Algeria using a probabilistic approach.

The research methodology followed in this study consisted of preparing a catalog of seismicity in the study area, delimiting source areas characterized by homogeneous seismicity, and using the attenuation of the peak acceleration to assess the probability distribution of peak accelerations at each site. The input parameters required by the CRISIS software package were estimated using the available seismic data to improve our understanding of seismicity rates in the area and to account for all high-magnitude earthquakes that could affect calculations of the seismic hazard.

Seismicity catalog

The catalog used for this work is a compilation of seismic data from Northeast Algeria from several sources. The main source is the seismic catalog of Harbi et al. (2010), which covers seismicity in Northeast Algeria between 3°–8°E and 33°–38°N. Other sources used for our catalog include CRAAG (1994), covering seismicity in Algeria during the period 1365–1992, which uses data from IMPGA, BCISC, and Benhallou (1985) as principal sources; Benouar and Perkins (1993), Benouar (1994), which covers the entire Maghreb region from 1900 to 1990 and uses Mezcuca and Martinez Solares (1983) as its main data source; IGN (2005), which covers the Ibero-Maghreb Region for the period 412–2005; Mokrane (1994), which covers the period 1365–1992; and USGS NEIC data files (1992). Data from the International Seismological Center (ISC) from the period 1950–2015 were also used to improve instrumental seismicity and complete the catalog of magnitude estimates.

To compile a catalog for our study area, we followed three steps: we sought historical data for the period 419–1900, included instrumental data after 1900, and obtained relevant data from the catalog compiled for all of Algeria.

The raw catalog contains 4703 events, covering the period between 1830 and the end of 2015; of these, 1707 have no

magnitude and 561 (M note defined). The minimum magnitude is M_s 2.0; i.e., the catalog consists only of earthquakes greater than M_s 2.0.

Homogenization of the catalog

The compilation of a catalog from different sources is likely to include earthquake magnitudes calculated on different scales. Thus, we must homogenize magnitudes to a uniform scale before the seismic hazard can be estimated.

For historic seismicity, surface wave magnitudes M_s were calculated by Benouar (1994) from epicentral intensity, and the same author evaluated the relationship between M_s and m_b for the Ibero-Maghreb region. Because many events use local magnitude (ML), it is necessary to convert to M_s , yet when we attempt to quantify the empirical relationship between M_s and ML, as illustrated in (Fig. 3), magnitudes (M_s) tend to be underestimated. To remedy this problem, the conversion made by Ambraseys (1985) and Benouar (1994) are used, applied to moderate seismicity, and calculated for the Maghreb region, respectively.

Completeness analysis

Evaluation of historic records and instrumental earthquakes shows that the magnitude distribution of the seismic catalog is not homogeneous over time (Fig. 4). The further back in time, the higher the lowest recorded magnitude. To obtain real rates of occurrence for MFDs (magnitude–frequency distributions), a date at which the catalog is complete must be determined for each magnitude. A perfect estimate of the annual rate of seismicity in a source region requires a complete catalog, i.e., one in which all

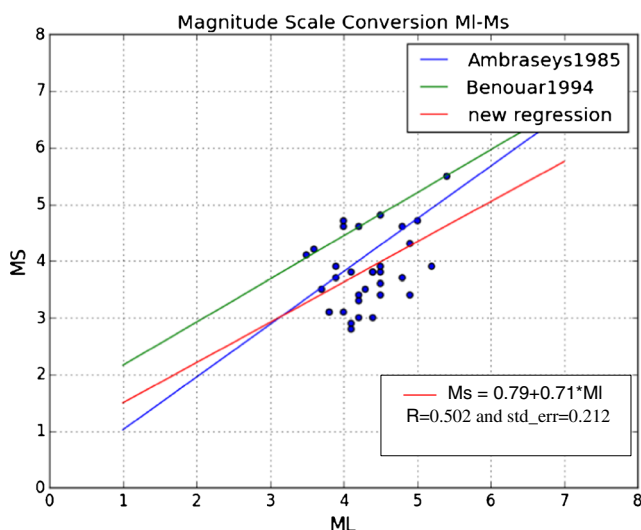


Fig. 3 Comparison of conversion relation for local magnitude (ML) to surface wave magnitude (M_s)

earthquakes are reported. For this purpose, the magnitudes of earthquakes and years of occurrence were used to estimate the year from which the catalog could be considered complete with respect to each magnitude. Figure 4 shows a completeness analysis using the cumulative visual (CUVI) method (Mulargia and Tinti 1987) applied to the Eastern Algeria earthquake catalog. Accordingly, we determined a threshold magnitude of 2.4 for completeness, but the corresponding catalog completeness varied by source region (Table 1 and Fig. 4) when applied to data from the earthquake catalog of Eastern Algeria. Accordingly, a 2.4-threshold magnitude and various years were selected from which we observed complete earthquake catalogs of source zones.

Declustering (removing aftershocks)

In the probabilistic approach, earthquakes are expected to occur as a Poisson process; i.e., random and stochastically independent in time and space (Gardner and Knopoff 1974). A Poisson process is used to describe the occurrence of the main shock and aftershocks of every major earthquake sequence. Indeed, designations such as “foreshock” and “aftershock” depend on the major event to which smaller earthquakes are related.

We used a Python program called Cluster, based on Gardner and Knopoff (1974), to remove aftershocks. This program groups interdependent earthquakes on the basis of their proximity in time and space. Thus, we removed interdependent earthquakes from each group, keeping only the event with the largest magnitude.

In what follows, the calculations and necessary steps for estimating the seismicity parameters are carried out on complete parts of each regional catalog which include only independent events in each source area.

A final parameter in window-based declustering method is the ratio between foreshock and aftershock time window or f/a ratio. We evaluated the time impact of this parameter along with the choice of declustering window. The results for four f/a ratio ranging between 0.25 and 1 in Table 2 indicate that a large f/a ratio results in more earthquakes being removed, but it is difficult to decide which value is more appropriate. We settled on a value of 0.5 for this parameter.

Figure 5a and b shows the results of declustering with the linked-window method, Gardner and Knopoff window and a ratio f/a of 0.5.

Fig. 4 CUVI (cumulative visual) completeness analysis for different ranges of lower magnitude. The **bold red line** corresponds to the completeness date being evaluated; the **dashed red line** corresponds to the next more recent completeness date. The **dashed black line** corresponds to the lowest magnitude that does not show a change in rate (knick point) beyond the completeness date from period 1830–2015

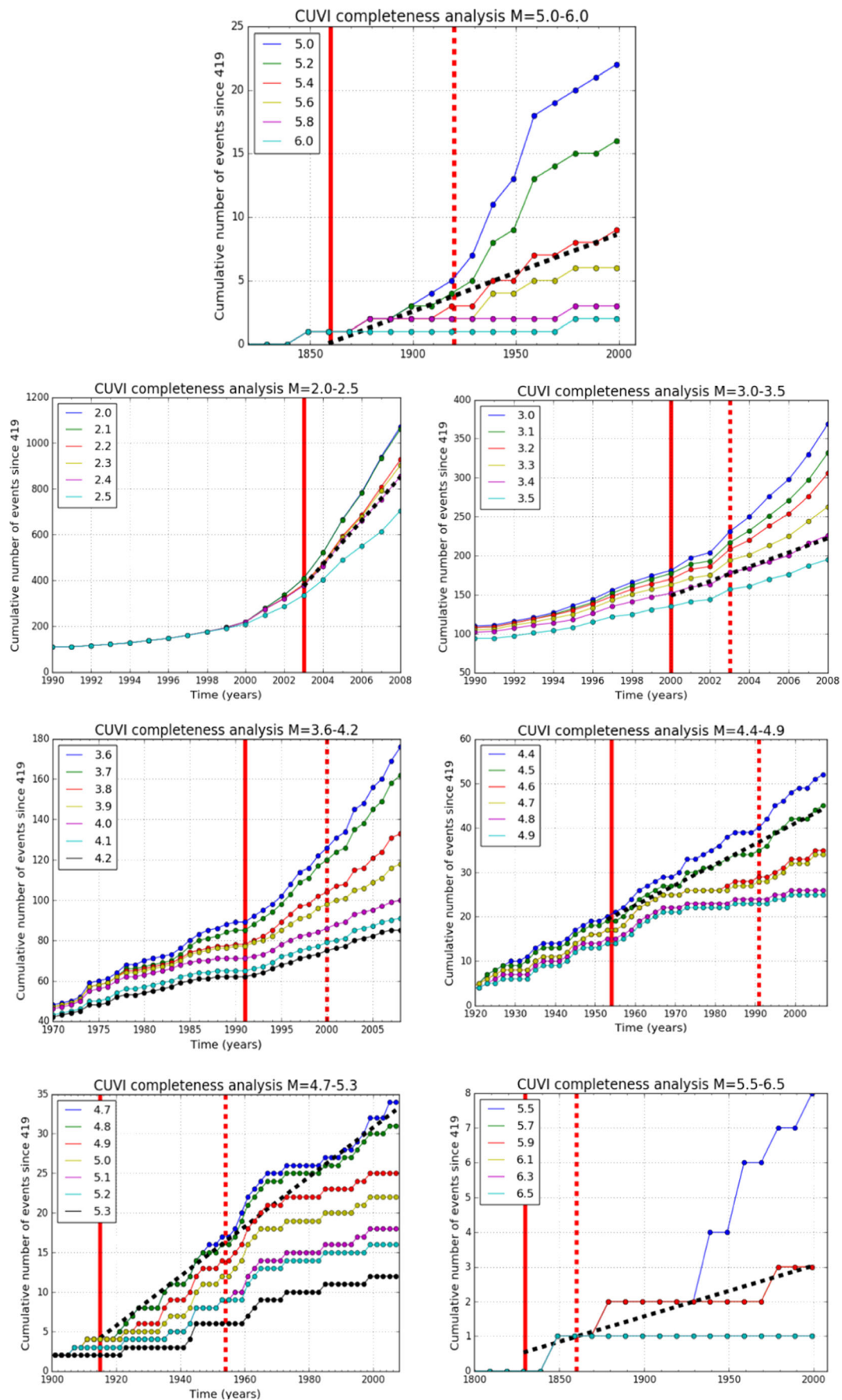


Table 1 Results of the completeness analyses (period 1830–2015)

Interval magnitude	Completeness period	Number of earthquakes for completeness	Year of completeness	Magnitude completeness
[5.5–6.5]	1830–2003	3	1830	5.9
[5.0–6.0]	1860–2003	9	1860	5.4
[4.7–5.3]	1915–2003	53	1915	4.8
[4.4–4.9]	1954–2003	46	1954	4.5
[3.6–4.2]	1991–2003	149	1991	3.8
[3.0–3.5]	2000–2003	148	2000	3.4
[2.0–2.5]	2003–2015	635	2003	2.4

Definition of the seismic source areas

In seismic hazard assessment, the definition of source areas (or seismogenic zones) is based on the knowledge of active tectonics (Fig. 1) and the seismicity in the study area (Fig. 2). In regions of diffuse seismicity, areas that represent potential earthquake sources can be modeled as being homogeneous with respect to crustal thickness, geodynamic stress field, and earthquake distribution. In this study, the adopted zoning convention extends the seismogenic sources to match previous seismic hazard studies (e.g., Aoudia et al. 2000; Harbi et al. 2007; Mourabit et al. 2014). A slight change was made in the demarcations of the source areas to maximize the number of earthquakes in the region bounded by 33°–38°N, 4°–9°E. This rezonation divides the region into seven polygonal source areas; earthquakes belonging to each source were selected. Figure 6 was compiled using the general earthquake catalog to create a subcatalog for each source area that characterized its seismic activity. The following subsections provide a general description of each source region (Fig. 7).

The Babors (Z1)

The Babor Mountains extend east from Soummam Valley in the eastern Akbou massif, part of the Petite Kabylie, to the meridian of Jijel (Fig. 1). This area is divided into several tectonic units (from the north to south): Brek, Gouraya and

Draa El Arba, Erraguene, Babors, and Beni Ouartilane (Harbi et al. 2003; Beldjoudi et al. 2009). The dominant rocks are

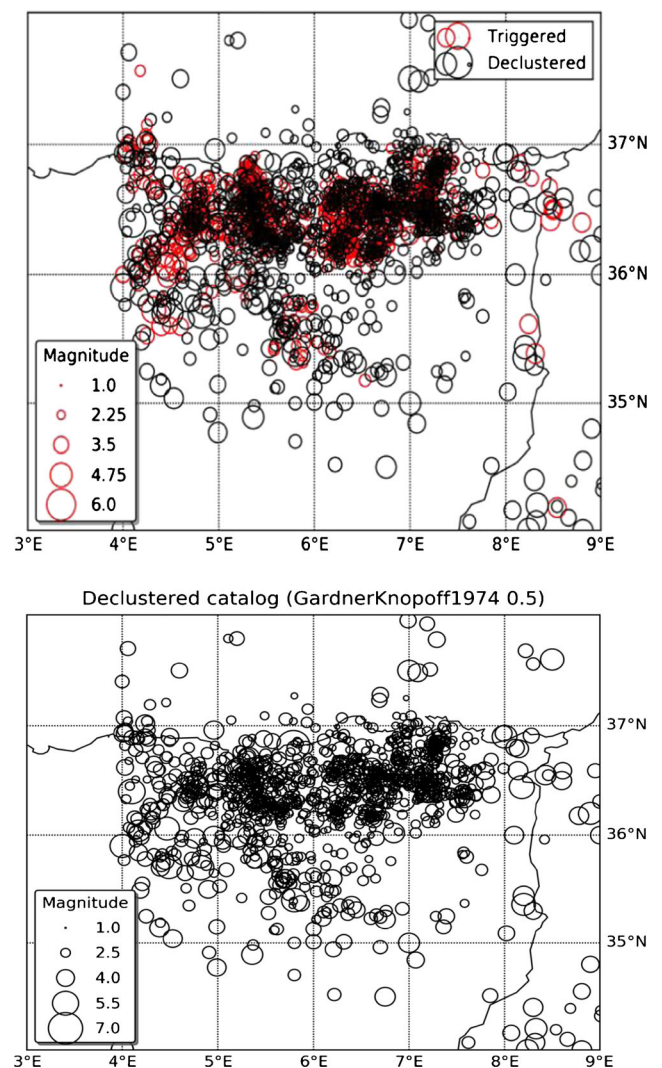
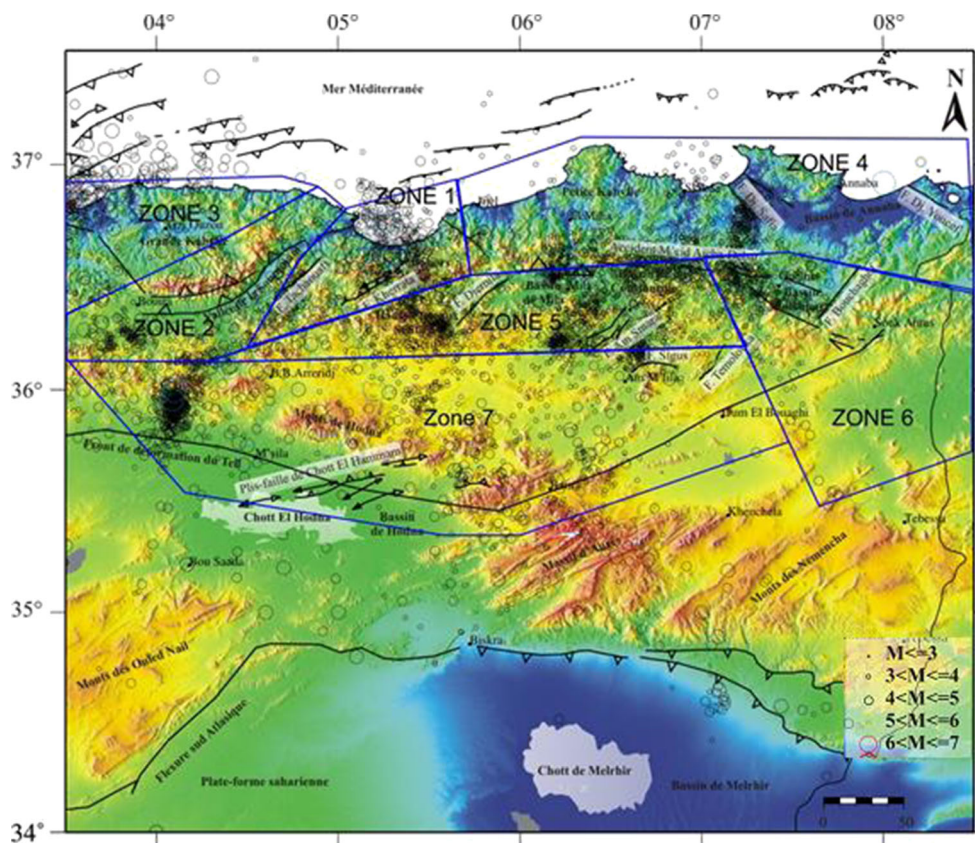


Fig. 5 a Map of merged northeastern part of Algeria catalog using before and after declustering (red circle triggered events, black circle declustered events). b Map of declustered catalog after application the completeness constraint (linked-window method, Gardner–Knopoff 1974 window; and f/a ratio of 0.5, 1511 events declustered through 2435)

Table 2 Number of earthquakes after declustering for different declustering windows of Gardner–Knopoff (GK) and foreshock/ aftershock window ratios (f/a ratio) of 0.25, 0.5, 0.75, and 1.00

f/a ratio Gardner–Knopoff	Whole northeastern catalog (2445 earthquakes)			
	0.25	0.5	0.75	1
Number of earthquakes after declustering	1586	1511	1467	1421

Fig. 6 Seismotectonic zoning adopted in the northeastern part of Algeria, dressed on the basis of previous works (Audia et al. 2000; Mourabit et al. 2014)



Jurassic and Cretaceous carbonates, comprising dolomites, limestones, and marls. Seismic activity in this region is generally moderate and diffuse. However, on 17 February 1949, a Ms 4.7 earthquake (intensity VII, (MSK)) occurred near the village of Kherrata, causing serious damage. Rothé (1950) located the epicenter at 36°30'N, 5°15'E and observed that the trace of the fault surface, striking N070-E, is likely associated with an active asymmetric fold in the area (Meghraoui 1988). This fault–fold pair seems to be responsible for the constant seismic activity in the Babors. This area has recorded hundreds of earthquakes, a few dozen of which have magnitudes $4.0 \leq M_s \leq 5.9$.

Offshore area (Z4)

Tectonic activity in the study area is marked by continental faults that could extend to sea level, the marine environment such as the faults of Cape Rosa West of El Kala, Djebel Safia East of Skikda, and Azemmour in the Collo Massif (Harbi et al. 2010).

Two major earthquakes occurred offshore of the town of Jijel on 21 and 22 August 1856 (intensities of IX and X (MSK), respectively), with epicenters located at approximately 37°1'N, 5°E (Rothé 1950). A tsunami followed the first shock, causing flooding and serious damage to surrounding communities (Ambraseys 1982; Harbi et al. 2011). The

isoseist curves are elongated NE–SW (relative to E–W), indicating an active structure in this orientation, probably located on the continental shelf, although this remains to be confirmed (Meghraoui 1988). The seismicity map shows earthquakes concentrate north of Skikda. Indeed, a few dozen are offshore, while others are marine faults. The best-known marine earthquake occurred offshore from Djidjelli in 1856 (Harbi et al. 2011). An Ms 4.9 earthquake struck north of Philippeville (Skikda) in 1935 with intensity VI (MSK), and an Ms 5.0 earthquake struck northeast of El Kala (intensity VI, MSK) in the same year.

Soummam zone (Z2)

The western end of the Babors is marked by the Soummam Valley, an elongated Neogene Basin that contains clearly observable large-scale geological structures. Seismic activity is moderate but continuous. According to Boudiaf (1996), analysis of a Digital Terrain Model (DTM) of the area and aerial photographs of the region shows recent tectonic structures. In the Tazmalt–M'chedallah region, alluvial terraces are significantly distorted by tectonic escarpments, affecting the Quaternary glacia; these movements are also visible in the region of Sidi Aich. It is noteworthy that the Pliocene strata are widely deformed throughout the Soummam Basin. In terms of seismic history, the Pliocene strata in the Soummam

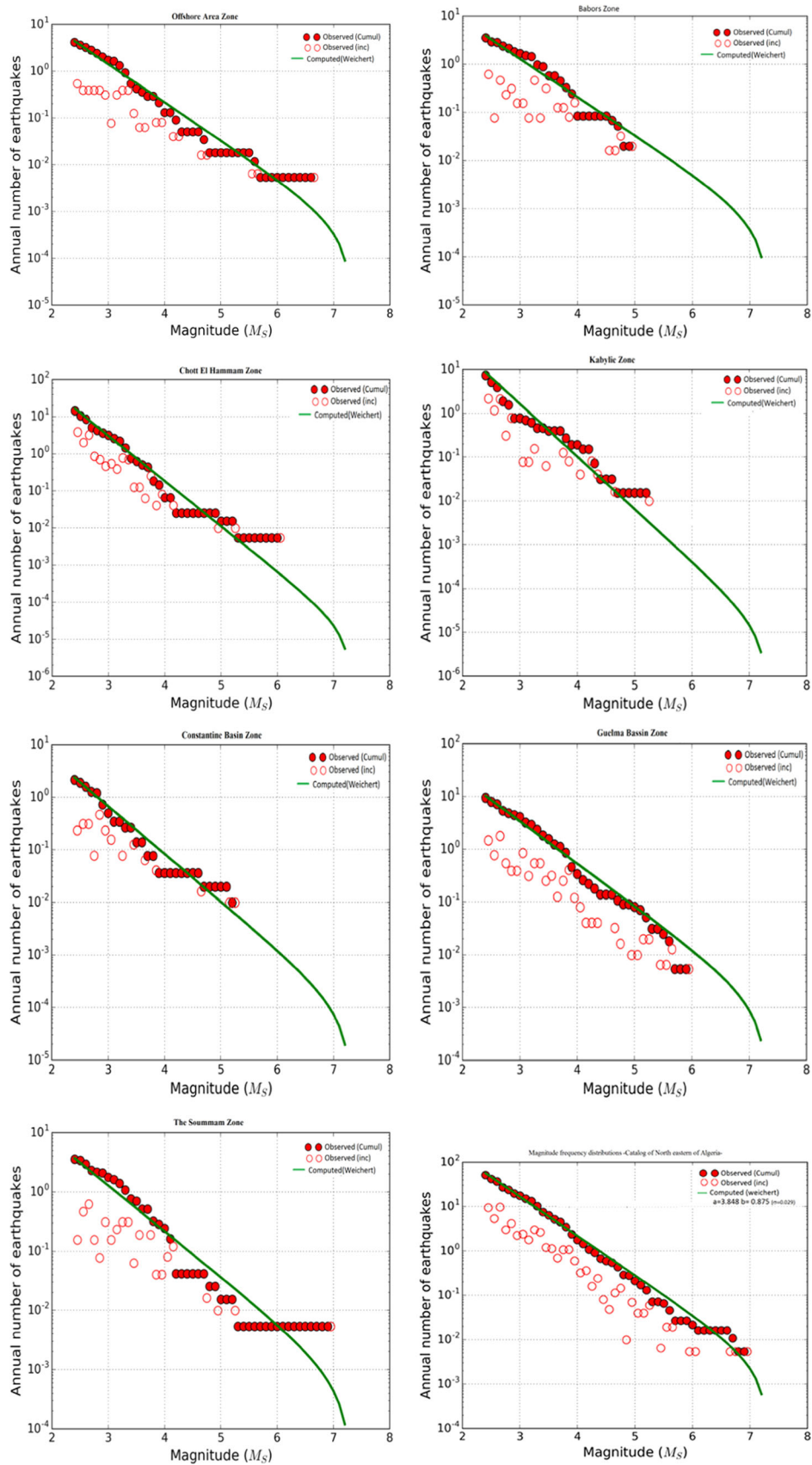


Fig. 7 Observed and computed MFD for the merged Northeastern Algeria catalog and sources area

region reported by Hée (1933, 1950), Rothé (1950), Mezcuca and Martinez Solares (1983), and Ambraseys and Vogt (1988) seem to be the site of many destructive earthquakes in the 200 years prior to 1910 (Harbi et al. 2010).

Kabylie zone (Z3)

The area of Kabylie is characterized by high alpine mountains in a structurally complex environment. Thrusts underlain by nappe fronts involving basement rocks strike roughly east–west with vergence to the south (Aoudia et al. 2000). There is no geological or morphological evidence of recent seismic activity in this area. This zone is considered to have a low degree of seismic activity relative to neighboring areas.

Constantine Basin (Z5)

An M 6.0 earthquake struck the Constantine region in 1985. Seismic and tectonic investigations have shown that ancient and recent seismic activity in this area is linked to the presence of a sinistral strike–slip fault striking N55–E (Bounif et al. 1987). Compared with the many intra-mountain basins of the Tell, the Constantine Basin occurs at higher altitudes and exhibits a different faulting mechanism to that of the four above-mentioned zones. Its geomorphology is characterized by deep and narrow valleys with steep slopes. Field investigations and conventional geological maps show the existence of active faults. Many of these faults trends NE–SW, which is the orientation of the surface, ruptures that formed from the largest seismic event in this region (Guiraud 1977).

Guelma Basin (Z6)

The Guelma zone shows a different faulting mechanism from those described above. Meghraoui (1988) described in this region a pull-apart basin that formed between two overlapping east–west dextral strike–slip faults. Crustal extension occurs between the faults. The size of the pull-apart is important and is linked to the amount of overlap (25 km) and distance between overlapping fault segments (Aoudia et al. 2000). The ends of the pull-apart basin are marked by a N–S to NNW–SSE bounding normal fault system that intersects the subparallel shear faults.

In this basin, the Bouchegouf and Hammam N’Bailis faults have particularly interested geologists. These faults offset Quaternary deposits and are related to hydrothermal activity, which accounts for the movement on these faults (Vila 1980).

The largest seismic event in this area occurred on 10 February 1937 ($M_s = 5.2$; Benouar and Perkins 1993). Two destructive earthquakes of intensity VIII (MSK) struck the region on 17 June 1908 and 3 December 1928.

Chott El Hammam (Z7)

Two moderate to major earthquakes have affected this region. The most recent was an M 5.5 on 1 January 1965 that caused serious damage in the city of Msila (Roussel 1973). Previously, an intensity IX (MSK) earthquake struck the area on 12 February 1946 (35°45’N, 4°57’E). Rothé (1950) and Meghraoui (1988) associated these seismic events in the region with the 1965 Msila event, where E–W asymmetric folds indicating transport to the south and that underlying faults that cut Pliocquaternary units in this region dip to the north, indicating in turn a relationship between seismic activity and the reverse fault at Chott El Hammam. The NNE extension of the Chott El Hammam fold–fault line is represented by the Boutaleb fold, which is linked to reverse faulting with an overlap of ante-Neogene substrata on its southeast side (Meghraoui 1988). Regarding the fold at Chott El Hammam, Guiraud (1971) indicated the presence of a folded forward slope dating back to the Pleistocene (Tensiftien, 200,000 years). The reverse fault bordering the slopes to the southeast of this fold is not visible on the surface, as it is covered by modern clayey–sandy deposits, though its length is estimated at 60 km. Its recent activity is confirmed by the intense seismic activity in this region (Meghraoui 1988).

In the Bibans, the Mansoura region appears to be relatively active. The most recent significant earthquake in this region was an $M_s = 5.1$ on 13 November 1974 with a maximum intensity of VII (MSK), although it has experienced stronger shocks previously (Harbi et al. 2010). This zone of generally low seismicity encompasses part of the Bibans and Boussaada at the southern boundary of the Hodna Basin (Harbi et al. 2010).

Choice of ground motion attenuation relationships

The choice of a ground motion prediction equation is a critical factor in the estimation of seismic hazard. In past decades, many attenuation relationships have been empirically derived based on strong-motion data sets from different regions; however, in regions characterized by moderate seismicity, the amount of strong motion data is generally insufficient for such an approach. No such attenuation law has been proposed for Algeria. For this study, the relationships of Ambraseys et al. (1996) and Berge-Thierry et al. (2003) were chosen for two reasons, as follows. (i) Each model presents three different equations, each related to one of the three major types of faults: reverse, normal, and strike–slip. These relations vary according to three main factors: magnitude, distance, and signal frequency. In our data set, the strongest accelerations are for earthquakes dominated by reverse faulting. (ii) The relationships of Ambraseys et al. (1996) and Berge-Thierry et al.

(2003) were developed from European event data, and they can be applicable to our case study.

The attenuation relationships of Ambraseys et al. (1996) and Berge-Thierry et al. (2003) are not completely independent because many events were used by both works. Both relationships were determined for crustal earthquakes with focal depths of ≤ 30 km, are expressed in terms of M_s (surface wave magnitude), and are valid for magnitudes $4 \leq M_s \leq 7.5$. However, there are also a number of differences. In this study, these equations are applied to bedrock. The relationship of Berge-Thierry et al. (2003), which is most recent, applies to M_s and hypocentral distances; it was chosen for comparative purposes. The selected events and the parameterization of the relationship have been adapted to the seismic context of the study region.

Figure 8a shows both attenuation relations for PGA, and Fig. 8b shows the spectral form of both attenuation laws for a fixed distance.

Results

Statistical evaluation of seismicity parameters

Modeling of the Gutenberg–Richter relation

The Gutenberg–Richter relation (Gutenberg and Richter 1944) relates the exponential temporal decrease in the number of earthquakes to earthquake magnitude, written in logarithmic form as

$$\log_{10}(N) = a - b \times M, \tag{1}$$

where N is the number of earthquakes with a magnitude greater or equal to M , and the factors a and b are Gutenberg–Richter parameters.

The method involves choosing a variable with different magnitudes between the minimum magnitude (M_{min}) in the seismic catalog of the area and calculating the cumulative number of earthquakes of magnitude higher or equal to each selected value. The evaluation of the parameters a and b of the Gutenberg–Richter law for each of the source area is performed by plotting the regression line that adjusts points on the curve described in relation (2) using the maximum likelihood solution MLS (Fig. 7). The values of these parameters are presented in the second and third columns in Table 3, with their corresponding standard deviations in columns 6 and 7.

Frequency of occurrence

The frequency of occurrence is the annual number of earthquakes with a magnitude greater than or equal to the catalog completeness magnitude. The frequencies of seismic

occurrence estimated for each source area are expressed in terms of the parameters λ and β of the equation

$$\lambda(M) = \lambda_0 \frac{e^{-\beta M} - e^{-\beta M_u}}{e^{-\beta M_0} - e^{-\beta M_u}} \tag{2}$$

where λ_0 is the exceedance rate of magnitude M_0 , β is a parameter equivalent to the b value for the source, and M_u is the maximum magnitude for the source.

The results for these parameters are summarized in Table 2.

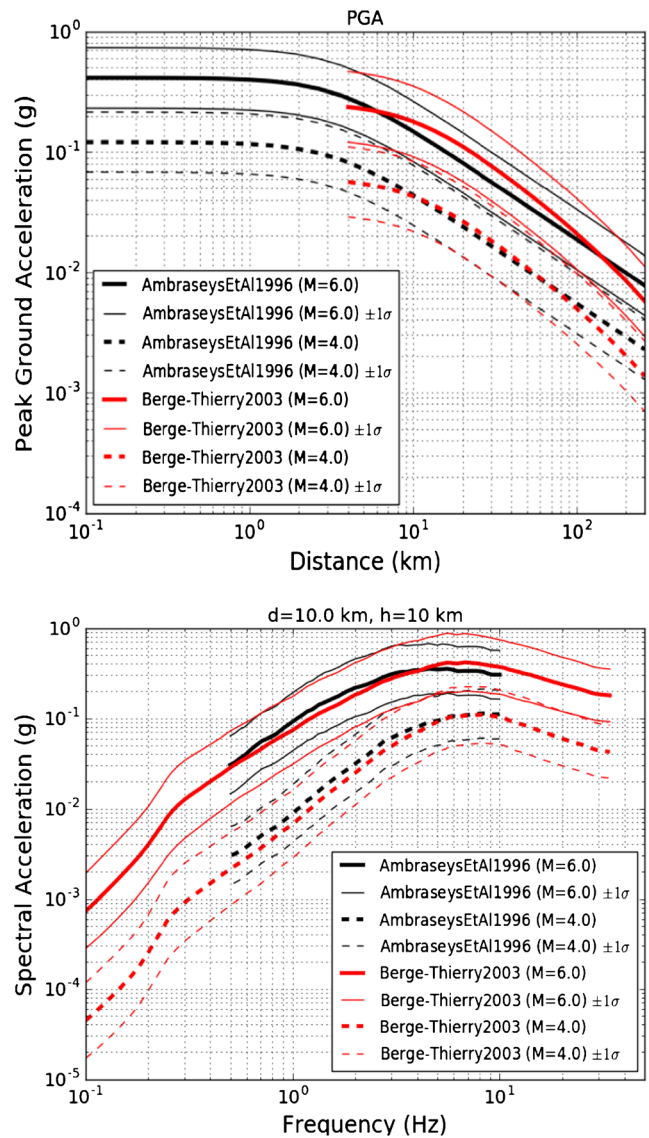


Fig. 8 a Comparison between PGA attenuation relations of Ambraseys et al. (1996) and Berge-Thierry et al. (2003). For $M_s = 4$ and $M_s = 6$ earthquake (hypocentral depth in the Berge-Thierry relation is 10 km). b Spectral attenuation relations of Ambraseys et al. (1996) and Berge-Thierry et al. (2003) for $M_s = 4$ and $M_s = 6$ earthquakes at Joyner-Boore, respectively, epicentral of 10 km. Hypocentral depth in the Berge-Thierry relation is set at 10 km. Note that the two relations should not be directly compared, due to their different distance metric

Table 3 The values of parameters a and b of the Gutenberg–Richter settings (calculated from the Weichert method (1980))

Source area zone	a	b	λ	β	σ_a	σ_b
The Babors (Z1)	2.493	0.794	0.207	1.829	0.059	0.064
Offshore area (Z4)	2.598	0.816	0.215	1.880	0.056	0.062
The Soummam (Z2)	2.421	0.771	0.217	1.776	0.059	0.063
The Kabylie (Z3)	3.811	1.200	0.103	2.763	0.043	0.089
Constantine Basin (Z5)	2.549	0.907	0.083	2.088	0.078	0.102
Guelma Basin (Z6)	2.938	0.803	0.532	1.849	0.036	0.040
Chott el Hammam (Z7)	4.139	1.219	0.184	2.806	0.031	0.066

Calculation of seismic hazard

For a given acceleration value, the CRISIS program calculates the annual probability of exceedance at a given site. In this

study, the probability of exceedance was set to 10% in a 50-year window to calculate the expected maximum acceleration values at a confidence level of 90%, corresponding to an estimated return period of 475 years. The maps produced by these estimates are contoured by peak ground acceleration (PGA).

Hazard curves and probabilistic spectra

A. Hazard curves From the accelerations obtained, it is possible to obtain area curves at any point. These combine the value of the annual rate of overrun with an acceleration. By inversion of this rate, it is possible to obtain the period of return for an acceleration greater than or equal to a given value. The hazard curves (Fig. 9a and c) were calculated for the five main towns in the region (Setif, Constantine, Bejaia, Jijel, and Kherrata).

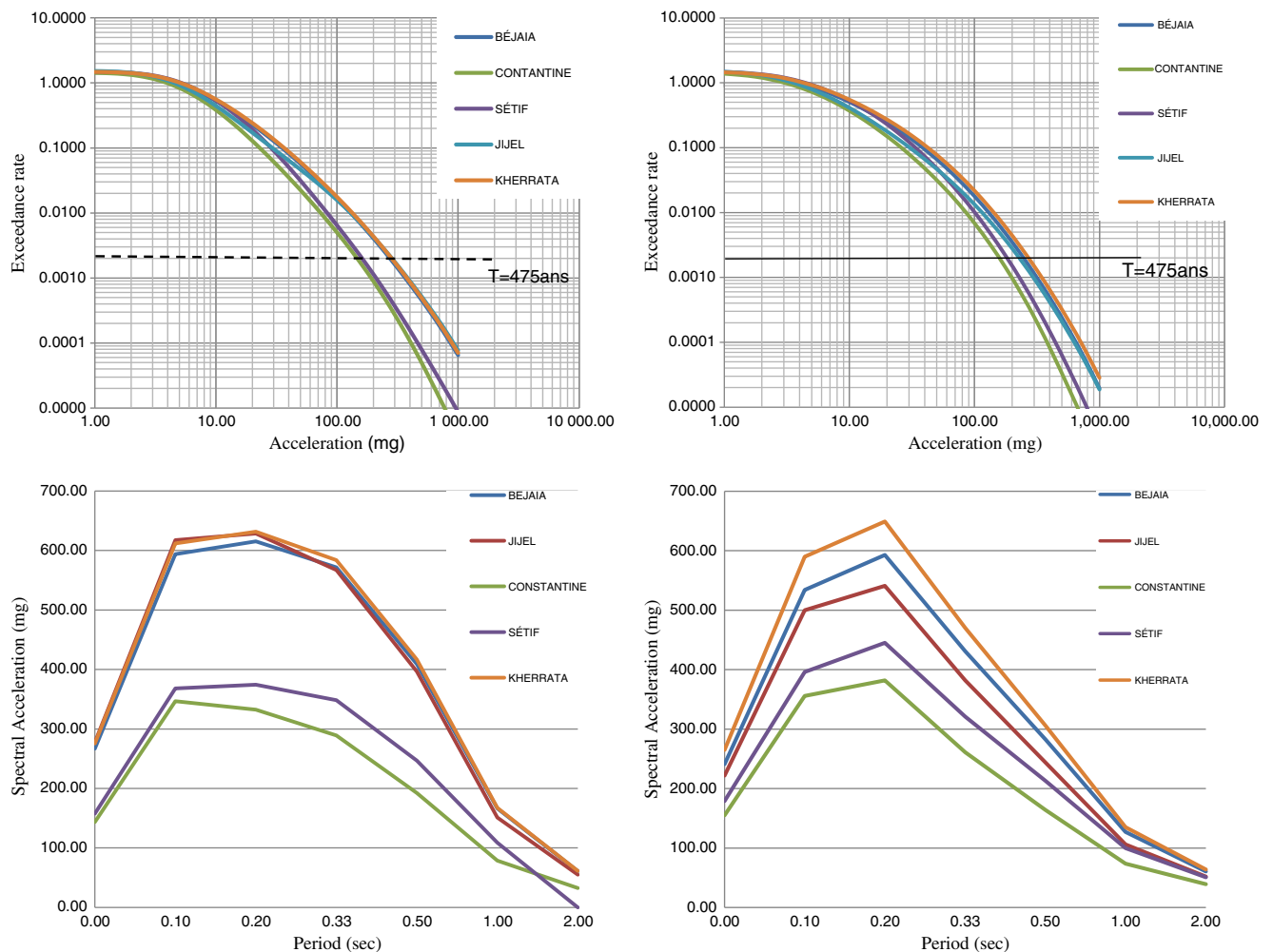
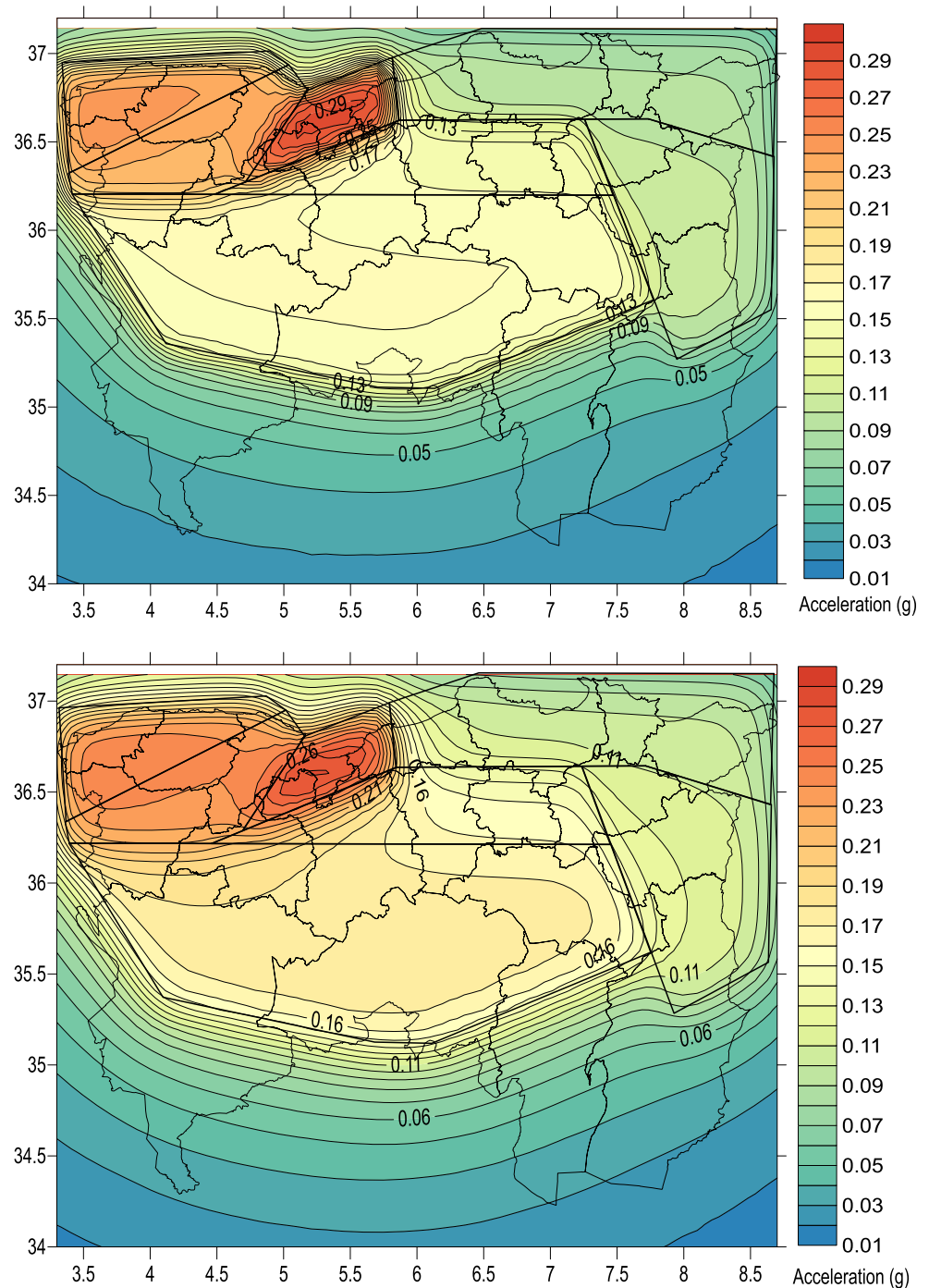


Fig. 9 a Hazard curve (Ambraseys et al. 1996 attenuation law). b Probabilistic spectrum (Ambraseys et al. 1996) attenuation law). c Hazard curve (Berge-Thierry et al. 2003 attenuation law). d Probabilistic spectrum (Berge-Thierry et al. 2003 attenuation relation)

Fig. 10 a Hazard map of Northeastern Algeria for a return period equal to 475 years, an annual probability of exceedance equal to 2×10^{-3} (calculated with Ambraseys et al. 1996 attenuation law). b Hazard map of Northeastern Algeria for a return period equal to 475 years, an annual probability of exceedance equal to 2×10^{-3} (calculated with Berg-Thierry 2003 attenuation law)



B. Specter of hazard uniform The uniform hazard spectra are plotted using the acceleration values calculated for different periods. They associate an acceleration value with a given period. They do not represent the spectrum of an actual earthquake but the levels of accelerations that are reached or exceeded for a return period of 475 years and for each spectral period. The period and frequency spectra are defined for a return period of 475 years and calculated for the five cities listed above (Fig. 9b and d).

Hazard maps for Northeast Algeria

Figure 10a presents the results of this study in the form of maps of peak horizontal acceleration values in %g, where g is acceleration due to gravity at sea level. Each area is characterized by an acceleration value with a 90% chance of non-exceedance during an observation window of 50 years. The models of Ambraseys et al. (1996) and Berge-Thierry et al. (2003) did not differ appreciably in the estimates of horizontal

peak accelerations. The “high” earthquake activity and zone dimensions of Z1 resulted in high hazard values. The estimated maximum PGA using the equations of Ambraseys et al. (1996) was ~290 mg, whereas the value estimated using Berge-Thierry et al. (2003) was ~260 mg. For hazard maps calculated from Ambraseys et al. (1996) and Berge-Thierry et al. (2003), with a return period of 475 years, acceleration estimates reached maximum values of 290 mg in areas with high seismicity rates and 30–90 mg in low-seismicity regions.

Discussion and conclusions

Probabilistic seismic risk maps were generated to estimate the probability of reaching or exceeding acceleration levels in Northeast Algeria for earthquakes with a recurrence interval of 475 years, or equivalent, with a probability of occurrence exceeding 10% over the next 50 years. For the seven areas described above, maximum PGA values range from 0.09 to 0.29 g.

The estimated PGA values for the towns of Bejaia, Setif, Constantine, Jijel, and Kherrata in Northeast Algeria are 0.23 g, 0.16 g, 0.14 mg, 0.25 g, and 0.29 g, respectively.

In the hazard maps (Fig. 10a and b), the regional risk is not uniform throughout the study area. It is higher in Babors and Djidjelli and gradually decreases towards the south and east, reaching minima in the extreme east (e.g., Tebessa, Souk Ahras, and Etaref) and towards Chott El Hammam in the south.

The assessment of the seismic hazard in Northeast Algeria carried out in this study is a concrete, qualitative, and quantitative result established specifically for this region. It was calculated for firm soils, for a return period of 475 years. The resulting accelerations confirm that the region contains a zone of moderate seismic risk in Babors and Djidjelli and low risk in the south and east, namely in Souk Ahras, Tebassa, and Annaba in the east and in Batna, Biskra, and Msila in the south.

The present results are consistent with classifications of the seismic hazard in north Algeria reported by Audia et al. (2000), Pelaez et al. (2003, 2005), and Mourabit et al. (2014). The reported accelerations decrease from west to large Kabylie and from the east to south of Babors and Djidjelli. These previous results are consistent with those of the present study.

The seismic map used for seismic zoning in Algeria places Northeast Algeria in a moderate seismic zone with g values of 0.05 to 0.29, consistent with the maps of the present study (Fig. 10a and b).

In terms of disaster prevention, these maps (Fig. 10a and b) provide the maximum possible ground accelerations for each municipality in Northeast Algeria. They represent a basic tool

for decision-making in rural and urban planning and development through the correct application of the 1999 RPA.

Acknowledgements My sincere thanks and deep gratitude for availability, advice, and kindness go to the gentlemen: Thierry Camel Beek; Kris Vanneste and Bart Vlemminckx and all members’ seismology section of the Royal Observatory of Belgium that allowed me to enjoy the observation traineeship.

The authors warmly thank Professor Abdullah M. Al-Amri and two anonymous referees for their reviews and suggestions, which improved the manuscript.

References

- Ambraseys NN (1982) The seismicity of north Africa: the earthquake of 1856 at Jijel, Algeria. *Boll Geof Teorica App* 93:31–37
- Ambraseys NN (1985) Intensity-attenuation and magnitude-intensity relationships for northwest European earthquakes. *Earthq Eng Struct Dyn* 13:733–778
- Ambraseys NN, Vogt J (1988) Material for the investigation of the seismicity of the region of Algiers. *Earthquake Eng* 3:16–29
- Ambraseys NN, Simpson KA, Bommer J (1996) Prediction of horizontal response spectra in Europe. *Earthq Eng Struct Dyn* 25:371–400
- Aoudia A, Meghraoui M (1995) Seismotectonics in the Tell Atlas of Algeria: the Cavaignac (Abou ElHassan) earthquake of 25.08.1922. *Tectonophysics* 248:263–276
- Aoudia A, Vaccari F, Suhadolc P, Maghraoui M (2000) Seismogenic potential and earthquake hazard assessment in the Tell Atlas of Algeria. *J Seismol* 4:79–88
- Beldjoudi H, Guemache MA, Kherroubi A, Semmane F, Yelles-Chaouche AK, Djellit H, Amrani A, Haned A (2009) The Lâalam (Béjaïa, north-east Algeria) moderate earthquake ($M_w = 5.2$) on March 20, 2006. *Pure Appl Geophys* 166:623–640
- Bender BK (1987) SEISRISK III: A computer program for seismic hazard estimation, U.S. Geological Survey Bulletin. 1772
- Benhallou H (1985) Les catastrophes séismiques de la région d’Echelif dans le contexte de la sismicité historique de l’Algérie. Thèse d’Etat, USTHB, Alger
- Benouar D (1994) Materials for the investigation of the seismicity of Algeria and adjacent regions during the twentieth century. *Ann Geofis* 4:459–860
- Benouar D, Perkins DM (1993) The seismicity of Algeria and adjacent regions during the twentieth century, PhD thesis, Imperial College of Science, Technology and Medicine, University of London, p 712
- Berge-Thierry C, Cotton F, Cushing M, Griot-Pommer DA, Joly J, Levret A, Scotti O (2003) New empirical response spectral attenuation laws for moderate European earthquakes. *J Earthq Eng* 7(2): 193–222
- Boudiaf A (1996) Etude sismotectonique de la région d’Alger et de la Kabylie (Algérie) : Utilisation des modèles numériques de terrain (MNT) et de télédétection pour la reconnaissance des structures tectoniques actives: contribution à l’évaluation de l’aléa sismique. Thèse, Univ Montpellier II, France
- Bounif A, Haessler H, Meghraoui M (1987) The Constantine (northeast Algeria) earthquake of October 27/1985: surface ruptures and after-shock study. *Earth and Planet, Sc Lett* 85:451–460
- Cornell CA (1968) Engineering seismic risk analysis. *Bull Seism Soc Am* 58:583–1606
- CRAAG-Centre de Recherche en Astronomie, Astrophysique et de Géologie (1994) Les séismes en Algérie de 1365 à 1992. Service de surveillance sismique, Alger
- Gardner JK, Knopoff L (1974) Is the sequence of earthquakes in Southern California, with aftershocks removed, Poissonian? *Bulletin of the*

- Seismological, Society of America, 64 (5) Publisher: Seismological Society of America
- Guiraud R (1971) Aperçu sur les principaux traits structuraux du Hodna et des régions voisines. Publ Serv Géol Algérie, nlle série, Bull. n°41
- Guiraud R (1977) Sur la néotectonique des régions ouest constantinoises. Bull Soc Géol. France, N° 3:645–650
- Gutenberg B, Richter CF (1944) Frequency of earthquakes in California. Bull Seism, Soc Am 34:185–188
- Harbi A (2006) Evaluation de l'Aléa Sismique en Algérie du Nord par la Modélisation de l'Input Sismique dans les Zones Urbaines et l'Établissement d'un Catalogue. PhD Thesis, University of Algiers
- Harbi A, Bennour D, Benhallou H (2003) Re-appraisal of seismicity and seismotectonics in the north-eastern Algeria part I: review of historical seismicity. J Seismol 7:115–136
- Harbi A, Maouche S, Vaccari F, Aoudia A, Oussadou F, Panza GF, Benouar D (2007) Seismic input and site effects in the Sahel-Algiers region (North Algeria). Soil DynEarthquEng 27(5):427–447
- Harbi A, Peresan A, Panza GF (2010) Seismicity of eastern Algeria: a revised and extended earthquake catalogue. Nat Hazards 54:724–747
- Harbi A, Meghraoui M, Maouche S (2011) The Djidjelli (Algeria) earthquakes of 21 and 22 August 1856 (10VIII, IX) and related tsunami effects revisited. J Seismol 15:105–129
- Hée A (1933) La fréquence des tremblements de terre en Algérie 1911–1932. Monogr Bur Centr Seismol Intern. p 99
- Hée A (1950) Catalogues des séismes algériens de 1850 à 1911. Ann Phys Globe. Strasbourg 6:41–49
- McGuire RK (1976) Fortran computer program for seismic risk analysis, US Geological Surve, open-File Report, 76–67
- McKenzie DP (1972) Active tectonics of the Mediterranean region. Geophys J R Astron Soc 30:109–185
- Meghraoui M (1988) Géologie des zones sismiques du nord de l'Algérie, tectonique active, paléosismologie, et synthèse sismotectonique. PhD-Thesis, Univ. Paris-sud Orsay, p 356
- Mezcua J, Martinez Solares JM (1983) Sismicidad Del Area IberoMogrebi. Seccion de Sismologia, Inst Geogr Nacional, Madrid
- Mokrane A (1994) Les séismes en Algérie de 1365 à 1992. Publication du Centre de Recherche en Astronomie, Astrophysique et Géophysique, Département: Etudes et Surveillance Sismique, ESS, C.R.A.A.G, Alger-Bouzaréah
- Mokrane A, Ait Messaoud A, Sebai A, Ayadi A, Bezzeg-houd, M (1994) Les séismes en Algérie de 1365 à 1992. Publication du Centre de Recherche en Astronomie, Astrophysique et Géophysique, Département: Etudes et Surveillance Sismique, ESS, C.R.A.A.G, Alger-Bouzaréah, 277 pp
- Mourabit T, Abou Elenean KM, A Ayadi, D Benouar, A Ben Suleman, M Bouzzeghoud, A Heddadi, M Choutak, MN ElGabry et al (2014) Neo-deterministic seismic hazard assessment in North Africa. J Seismol. ISSN 1383–4649, 18(2)
- Mulgaria F, Tinti S (1987) Seismic sample areas defined from incomplete catalogs: an application to the Italian territory. Phys Earth Planet, Inter 40:273–300
- Ordaz MG, el Aguilar A, Arboleda J (2007) CRISIS2007—program for computing seismic hazard. Instituto de Ingeniería, Universidad Nacional Autónoma de México, UNAM, México
- Pelaez JA, Hamdache M, Lopez Casado C (2003) Seismic hazard in Northern Algeria using spatially-smoothed seismicity. Result for peak ground acceleration. Tectonophys 372:105–119
- Pelaez JA, Hamdache M, Lopez Casado C (2005) Updating the probabilistic seismic hazard values of Northern Algeria with the 21 May 2003 M 6.8 Algiers earthquake included. Pure Appl Geophys 162:2163
- Rothé JP (1950) Les séismes de Kherrata et la sismicité de l'Algérie. Bull Serv Cart Geol. Algérie, 4 ème série, Géophysique, N. 3, p 40
- Roussel J (1973) Les zones actives et la fréquence des séismes en Algérie 1716–1970. Bull Soc Hist Nat Afr Nord 64(3):11–227
- Vila, J. M (1980) La chaîne alpine d'Algérie orientale et des confins algéro-tunisiens. Thèse de Doctorat, Université de Pierre et Marie Curie (Paris VI), p 665
- Weichert DH (1980) Estimation of earthquake recurrence parameters for unequal observation period for different magnitudes. Bull Seismol Soc Am 70:1337–1346